Acta Crystallographica Section C
Crystal Structure Communications
ISSN 0108-2701

Disorder and conformational analysis of methyl β-D-galactopyranosyl-(1→4)-β-D-xylopyranoside

Wenhui Zhang, Allen G. Oliver and Anthony S. Serianni*

Department of Chemistry and Biochemistry, University of Notre Dame, 251 Nieuwland Science Hall, Notre Dame, IN 46556-5670, USA
Correspondence e-mail: aseriann@nd.edu

Received 4 August 2011
Accepted 14 November 2011
Online 6 December 2011

Methyl β-D-galactopyranosyl-(1→4)-β-D-xylopyranoside, $C_{12}H_{22}O_{10}$, (II), crystallizes as colorless needles from water with positional disorder in the xylopyranosyl (Xyl) ring and no water molecules in the unit cell. The internal glycosidic linkage conformation in (II) is characterized by a φ' torsion angle ($C2'_{Gal}-C1'_{Gal}-O1'_{Gal}-C4_{Xyl}$) of 156.4 (5)° and a ψ' torsion angle ($C1'_{Gal}-O1'_{Gal}-C4_{Xyl}-C3_{Xyl}$) of 94.0 (11)°, where the ring atom numbering conforms to the convention in which C1 denotes the anomeric C atom, and C5 and C6 denote the hydroxymethyl (–CH_2OH) C atoms in the β-Xyl and β-Gal residues, respectively. By comparison, the internal linkage conformation in the crystal structure of the structurally related disaccharide, methyl β-lactoside [methyl β-D-galactopyranosyl-(1→4)-β-D-glucopyranoside], (III) [Stenutz, Shang & Serianni (1999). *Acta Cryst.* C**55**, 1719–1721], is characterized by φ' = 153.8 (2)° and ψ' = 78.4 (2)°. A comparison of β-(1→4)-linked disaccharides shows considerable variability in both φ' and ψ', with the range in the latter (∼38°) greater than that in the former (∼28°). Inter-residue hydrogen bonding is observed between atoms $O3_{Xyl}$ and $O5'_{Gal}$ in the crystal structure of (II), analogous to the inter-residue hydrogen bond detected between atoms $O3_{Glc}$ and $O5'_{Gal}$ in (III). The exocyclic hydroxymethyl conformations in the Gal residues of (II) and (III) are identical (*gauche–trans* conformer).

Comment

The *N*-linked glycans of human glycoproteins are characterized by a common pentasaccharide core, $Man_3GlcNAc_2$, containing three D-mannose (Man) and two *N*-acetyl-D-glucosamine (GlcNAc) residues, with the terminal β-GlcNAc-(1→4)-β-GlcNAc portion linked to the L-asparagine side chains of the protein (Taylor & Drickamer, 2003). In contrast, the modes of attachment of *O*-linked glycans to proteins are more diverse, with *N*-acetyl-D-galactosamine, D-glucose, D-galactose, D-mannose or D-xylose covalently attached *via* the side chains of L-serine and L-threonine (Voet & Voet, 2011). For example, in the proteoglycans, chrondroitin sulfate polysaccharide chains are covalently attached to the core protein *via* a β-GlcA-(1→3)-β-Gal-(1→3)-β-Gal-(1→4)-β-Xyl tetrasaccharide (Xyl is xylopyranosyl), (I), with the terminal β-Xyl residue linked to L-serine (Nadanaka & Kitagawa, 2008). The residues comprising this linkage tetrasaccharide may be *O*-sulfated or *O*-phosphorylated. In this report, the crystal structure of the β-Gal-(1→4)-β-Xyl substructure of (I) has been determined in the form of its methyl glycoside, namely, methyl β-D-galactopyranosyl-(1→4)-β-D-xylopyranoside, (II). This new structure complements those of other structurally related β-(1→4)-linked disaccharides reported previously, including methyl β-D-galactopyranosyl-(1→4)-β-D-glucopyranoside, (III) (Stenutz *et al.*, 1999), methyl β-D-galactopyranosyl-(1→4)-α-D-glucopyranoside, (IV) (Pan *et al.*, 2005), methyl β-L-galactopyranosyl-(1→4)-β-D-glucopyranoside, (V) (Pan *et al.*, 2006), methyl β-D-galactopyranosyl-(1→4)-α-D-mannopyranoside, (VI) (Hu *et al.*, 2010), methyl β-D-galactopyranosyl-(1→4)-β-D-allopyranoside, (VII) (Zhang *et al.*, 2010), and methyl β-D-glucopyranosyl-(1→4)-β-D-glucopyranoside, (VIII) (Ham & Williams, 1970).

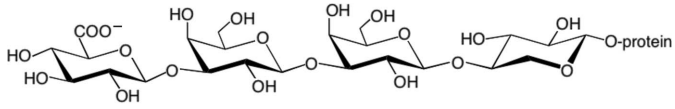

β-GlcA-(1→3)-β-Gal-(1→3)-β-Gal-(1→4)-β-Xyl,(I),linked to protein

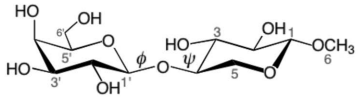

β-Gal-(1→4)-β-XylOCH$_3$,(II)

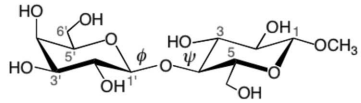

β-Gal-(1→4)-β-GlcOCH$_3$,(III)

Methyl β-D-galactopyranosyl-(1→4)-β-D-xylopyranoside, (II), was prepared by a chemical route (see *Supplementary material* for synthetic details). After purification by chromatography, (II) was crystallized from water to give microcrystals devoid of water. In this report, the crystal structure of (II) is compared with that of the structurally related disaccharide, methyl β-D-galactopyranosyl-(1→4)-β-D-glucopyranoside [methyl β-lactoside, (III); Stenutz *et al.*, 1999] (Table 2).

The crystal structure of (II) exhibits elements of disorder not observed in those of (III) and other β-(1→4)-linked disaccharides (Pan *et al.*, 2005, 2006; Hu *et al.*, 2010; Zhang *et al.*, 2010; Ham & Williams, 1970). This disorder is located exclusively within the Xyl residue, and modeling of the diffraction data yielded major (∼70%) and minor (∼30%) components; atoms in the latter are denoted with the suffix *A* throughout this article. The observed disorder has been attributed to an oscillation of the Xyl ring perpendicular to the plane of the ring, translating into librational motion across the β-(1→4) linkage. This behavior appears to be a characteristic feature of crystals of (II); data obtained from different

 doi:10.1107/S0108270111048347

samples of crystals yielded the same disorder. Why disorder in the glycosidic linkage appears in crystals of (II) and not in those of other β-(1→4)-linked disaccharides including (III) is unclear, but ring geometry and/or substituent effects in the Xyl ring, or packing considerations, probably play a role. The internal glycosidic linkages in other β-(1→4)-linked disaccharides are constrained by inter-residue hydrogen bonding between atoms O3 and O5′. The lack of an exocyclic –CH_2OH group in the Xyl ring of (II) may allow this hydrogen bonding in a wider range of linkage conformations, thus leading to linkage flexibility/disorder in the solid state. Whether this putative difference plays a functional role in the *O*-linkages of glycoproteins involving β-Xyl remains uncertain.

The presence of disorder in crystals of (II) complicates a quantitative analysis of molecular parameters such as bond lengths, angles and torsions due to averaging effects on the electron densities (and corresponding displacement ellipsoids) used to determine the structure. This fact is evident, for example, when comparing the C4—C5 bond length in (II) with that in (III), where a difference of ∼0.04 Å is observed (Table 2). In contrast, inspection of the X-ray structure of methyl β-xylopyranoside, (IX) (Takagi & Jeffrey, 1977), shows a C4—C5 bond of 1.519 Å, in better agreement with the corresponding value in (III) than in (II).

For the major component of (II), the C1—O6—C6 bond angle is 118.3 (9)°, statistically larger than the value of 113.7 (2)° found in (III), with the latter value similar to the corresponding value found in methyl β-xylopyranoside, (IX) (113.0°). In contrast, the internal C1′—O1′—C4 bond angle in (II) is 113.6 (7)°, similar to the corresponding value found in (III) [116.2 (2)°; Table 2]. This internal glycosidic bond angle is typically larger than that associated with the terminal methyl glycosides, presumably due to greater steric strain present in the internal linkage. The normal value of this angle in (II) suggests that the internal glycosidic torsion angles in (II) (*i.e.* φ' and ψ') are probably minimally affected by the presence of disorder in the Xyl residue. This conclusion is supported by the similar bond lengths observed in the Gal residues of (II) and (III) (Table 2).

Cremer–Pople (CP) puckering parameters for the pyranosyl ring constituents of (II) and (III) are shown in Table 3 (Cremer & Pople, 1975; Boeyens, 1978; Spek, 2009). The β-Gal ring in both structures adopts a chair conformation with similar θ and φ values, indicating similar degrees and directions for the slight distortion towards the $^{C3}TB_{C1}$ conformation (TB = twist-boat). The β-Xyl ring of (II) and β-Glc ring of (III) show the same degree of distortion, with the former slightly skewed towards $^{C3,O5}B$ (B = boat) and the latter towards $^{O5}TB_{C2}$. In contrast, the crystal structure of methyl β-D-galactopyranoside, (X) (Takagi & Jeffrey, 1979), has θ = 5.89° and φ = 346.6°, indicating a direction of distortion ($^{O5}TB_{C2}$) different from that in the Gal residues of (II) and (III). The CP parameters for methyl β-D-xylopyranoside, (IX), and methyl β-D-glucopyranoside, (XI) (Jeffrey & Takagi, 1977), are very similar (θ = 7–8° and φ = 36–38°), indicating a direction of distortion in (IX) similar to that in the Xyl reside of (II) but a direction of distortion in (XI) different from that

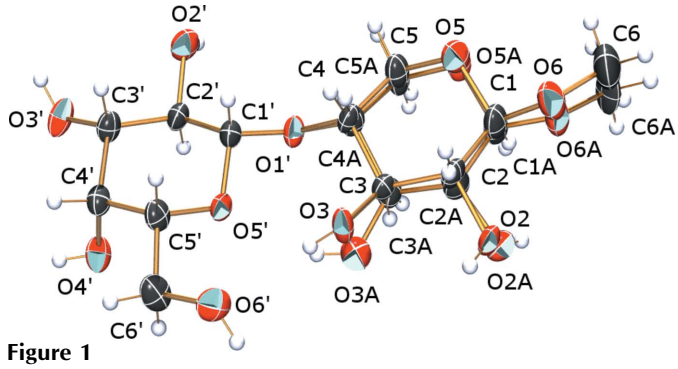

Figure 1
The molecular structure of (II), with atom numbering and showing both disordered components of the molecule. Displacement ellipsoids are depicted at the 50% probability level.

found in the Glc residue of (III). However, it must be noted that the distortion in (II) is highly dependent on the model used to treat the disorder. Examination of the electron-density map of the disorder shows no evidence for discrete regions of electron density corresponding to the separate components, so it is highly probable that the β-Xyl ring of (II) is dynamic, making the distortion difficult to quantify reliably.

The exocyclic hydroxymethyl conformations in the Gal residues of (II) and (III) are similar, with O5′—C5′—C6′—O6′ torsion angles near 60°, corresponding to the *gauche–trans* (*gt*) conformation. This behavior is similar to that found in methyl β-D-galactopyranoside, (X).

The internal glycosidic linkage conformation in (II) differs from that in (III), with the difference associated more with ψ' than with φ'; the φ' values differ by ∼3°, whereas the ψ' values differ by ∼16°. Table 4 summarizes the φ' and ψ' values observed in a series of β-(1→4)-linked disaccharides for which crystal structures have been reported. In this comparison, torsion angles involving heavy atoms were used to define φ' and ψ', namely, C2′—C1′—O1′—C4 for φ' and C1′—O1′—C4—C3 for ψ'. It is noteworthy that considerable variability in both φ' and ψ' is observed, with that for ψ' (37.7°) larger than that for φ' (28.4°). These findings, although confined to a relatively small data set, show that the stereoelectronic (*exo*-anomeric) effect does not severely constrain the φ' torsion angle in these linkages; presumably, crystal packing forces are strong enough to rotate the C1′—O1′ bond in order to minimize the packing energy. The comparatively greater variability in ψ' is presumably caused by different nonbonded (steric) effects that are structure-dependent, although packing forces may also contribute. Disaccharide (V) was excluded from this comparison since it contains an L-Gal residue and thus its internal glycosidic linkage is structurally distinct from the others.

Internal (inter-residue) hydrogen bonding occurs in (II) between atom O3 of the Xyl residue and atom O5′ of the Gal residue. The O3···O5′ internuclear distances of 2.729 (5) and 2.803 (13) Å (major and minor components, respectively) involving the two O3 (O3/O3*A*) positions show that two hydrogen-bonding geometries are possible; this observation suggests some plasticity in the overall conformation in accommodating this type of intramolecular hydrogen bond. It

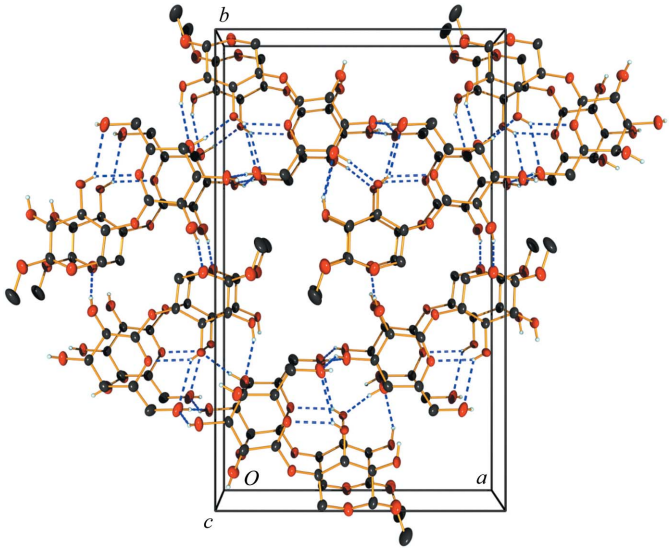

Figure 2
The hydrogen-bonding network for (II), viewed along the *c* axis. The minor disorder component has been omitted for clarity. Dashed lines represent hydrogen bonds.

is noteworthy that all of the disaccharides in Table 4 contain this hydrogen bond except (V) and (VII). The major-component hydroxy atom O3 also has a long inter-residue contact with hydroxymethyl atom O6′.

All hydroxy H atoms in the Gal moiety of (II) are involved as donors in intermolecular hydrogen bonds. In the Xyl residue, both atoms O2 and O3 are hydrogen-bond donors, whereas atom O2*A* is not well positioned to form a hydrogen bond with nearby acceptors. Atom O3 is involved as a donor in an inter-residue hydrogen bond with atom O5′. Atoms O1 and O2 of the Xyl residue are not involved as acceptors, whereas atoms O3 and O5 serve as mono-acceptors. Atoms O1′, O2′, O4′ and O5′ of the Gal residue are not involved as acceptors in intermolecular hydrogen bonds, while atom O3′ serves as a mono-acceptor.

The overall packing motif of (II) is a three-dimensional network of hydrogen-bonded molecules (Fig. 2). The interaction of atom O2′ with ring atom O5^{ii} forms chains related by the screw axis parallel to the *c* axis [symmetry code: (ii) $-x+\frac{1}{2}$, $-y+2$, $z+\frac{1}{2}$]. These chains are linked to other chains related by screw axes parallel to the *a* axis through the hydrogen bonds from atoms O4′ to O3^{iv}, O2 to O4′^{i} and O6′ to O3′^{i} [symmetry codes: (i) $x-\frac{1}{2}$, $-y+\frac{3}{2}$, $-z+2$; (iv) $x+\frac{1}{2}$, $-y+\frac{3}{2}$, $-z+2$]. These screw axes are translated along the *a* axis with respect to the others. Lastly, atom O3′ forms a hydrogen bond with atom O6′^{iii} related by the screw axis parallel to the *b* axis [symmetry code: (iii) $x+\frac{1}{2}$, $-y+\frac{3}{2}$, $-z+1$]. The disordered hydroxymethyl atom C6 and the minor component hydroxy atom O2*A* are oriented towards a void space within the lattice.

Experimental

The crystal structure of (II) was determined using a sample prepared chemically by the eight-step synthesis described in the *Supplementary materials*; the relevant literature references are: Schmidt & Michel (1985); Wu & Serianni (1991); Podlasek *et al.* (1995); Tropper *et al.* (1992); Gruzman *et al.* (2008); Ning *et al.* (2003). Disaccharide (II) was crystallized from water to give colorless needle-like microcrystals. Due to the growth of the compound as microcrystals, conservatively estimated at 10 µm in thickness, and the presence of only light atoms within the sample, synchrotron radiation was a necessity for the determination of the structure. Standard laboratory instruments only yielded data suitable for a low-quality preliminary structure.

Crystal data

$C_{12}H_{22}O_{10}$
M_r = 326.30
Orthorhombic, $P2_12_12_1$
a = 13.7878 (14) Å
b = 22.892 (2) Å
c = 4.6367 (5) Å
V = 1463.5 (3) Å^3
Z = 4
Synchrotron radiation
λ = 1.23990 Å
μ = 0.52 mm^{-1}
T = 150 K
0.08 × 0.01 × 0.01 mm

Data collection

Bruker APEXII diffractometer
Absorption correction: empirical (using intensity measurements) (*SADABS*; Sheldrick, 2008)
T_{min} = 0.566, T_{max} = 0.749
11197 measured reflections
2300 independent reflections
1900 reflections with $I > 2\sigma(I)$
R_{int} = 0.073
θ_{max} = 45.3°

Refinement

$R[F^2 > 2\sigma(F^2)]$ = 0.067
$wR(F^2)$ = 0.158
S = 1.16
2300 reflections
298 parameters
299 restraints
H-atom parameters constrained
$\Delta\rho_{max}$ = 0.35 e Å^{-3}
$\Delta\rho_{min}$ = −0.27 e Å^{-3}
Flack parameter: 0.6 (9), 920 Friedel pairs

Examination of the xylose moiety showed positional disorder in the peripheral atoms and close inspection of the displacement ellipsoids demonstrated that the entire ring was affected. The positions of the atoms in the major and minor components were determined initially by location of the major component and subsequent refinement of these sites at less than full occupancy, enhancing the difference Fourier map which displayed the location of the minor component atoms. The occupancies of the major and minor components were refined and summed to unity, yielding a 0.692 (9):0.308 (9) ratio. The minor component was restrained to have bond distances and angles similar to those of the major component to within a small error (s.u. = 0.02 Å or 0.02°). The major and minor components were both refined with anistropic displacement parameters, with displa-

Table 1
Hydrogen-bond geometry (Å, °).

D—H···A	D—H	H···A	D···A	D—H···A
O2—H2···O4′^{i}	0.84	2.27	2.997 (7)	146
O3—H3···O5′	0.84	2.09	2.729 (5)	133
O3—H3···O6′	0.84	2.48	2.978 (6)	119
O3*A*—H3*AA*···O5′	0.84	2.09	2.803 (13)	143
O2′—H2′···O5^{ii}	0.84	1.88	2.714 (9)	169
O2′—H2′···O5*A*^{ii}	0.84	2.03	2.86 (2)	169
O3′—H3′···O6′^{iii}	0.84	1.90	2.653 (5)	148
O4′—H4′···O3^{iv}	0.84	1.91	2.720 (6)	163
O4′—H4′···O3*A*^{iv}	0.84	2.01	2.795 (13)	154
O6′—H6′···O3′^{i}	0.84	1.85	2.678 (5)	169

Symmetry codes: (i) $x-\frac{1}{2}$, $-y+\frac{3}{2}$, $-z+2$; (ii) $-x+\frac{1}{2}$, $-y+2$, $z+\frac{1}{2}$; (iii) $x+\frac{1}{2}$, $-y+\frac{3}{2}$, $-z+1$; (iv) $x+\frac{1}{2}$, $-y+\frac{3}{2}$, $-z+2$.

Table 2
Comparison of structural parameters in (II) and (III).

gt stands for *gauche–trans*.

Bond distances and internuclear contacts (Å)	(II)†	(III)
C1—C2	1.495 (9)	1.516 (3)
C2—C3	1.519 (8)	1.519 (3)
C3—C4	1.518 (9)	1.531 (3)
C4—C5	1.489 (9)	1.530 (3)
C5—C6		1.508 (3)
C1′—C2′	1.530 (6)	1.527 (3)
C2′—C3′	1.529 (6)	1.531 (3)
C3′—C4′	1.535 (6)	1.521 (3)
C4′—C5′	1.520 (6)	1.521 (3)
C5′—C6′	1.516 (7)	1.511 (3)
C1—O1	1.373 (9)	1.384 (3)
C1—O5	1.444 (8)	1.413 (3)
C2—O2	1.413 (8)	1.418 (3)
C3—O3	1.424 (8)	1.421 (3)
C5—O5	1.443 (8)	
C6—O6		1.424 (3)
C1′—O1′	1.406 (5)	1.387 (3)
C1′—O5′	1.441 (5)	1.425 (3)
C2′—O2′	1.429 (6)	1.414 (3)
C3′—O3′	1.434 (5)	1.422 (3)
C4′—O4′	1.417 (6)	1.423 (3)
C5′—O5′	1.452 (6)	1.432 (3)
C6′—O6′	1.439 (5)	1.426 (3)
C4—O1′	1.443 (17)	1.437 (3)
O3···O5′	2.729 (5)	2.764 (2)
O3···O6′	2.978 (6)	
Bond angles (°)		
C1′—O1′—C4	113.6 (7)	116.2 (2)
C1—O1—C6	118.3 (9)	113.7 (2)
Torsion angles (°)		
C2—C1—O1—C6 (φ)	164.5 (9)	164.2 (2)
O5—C1—O1—C6 (φ)	−81.4 (11)	−77.4 (3)
C2′—C1′—O1′—C4 (φ')	156.4 (5)	153.8 (2)
O5′—C1′—O1′—C4 (φ')	−85.7 (6)	−88.4 (2)
C1′—O1′—C4—C3 (φ')	94.0 (11)	78.4 (2)
C1′—O1′—C4—C5 (φ')	−141.6 (8)	−161.3 (2)
H1′*A*—C1′—O1′—C4 (φ')	34.3	31.9
C1′—O1′—C4—H4*A* (φ')	−25.2	−43.7
O5′—C5′—C6′—O6′ (φ')	60.7 (5) (*gt*)	57.4 (2) (*gt*)

† Only parameters pertaining to the major component are reported.

Table 3
Cremer–Pople puckering parameters in (II), (III) and (IX)–(XI)†.

Compound	θ (°)	φ (°)	Q (Å)	q_2 (Å)	q_3 (Å)
(II), βGal*p*	7.3 (5)	14 (4)	0.596 (5)	0.078 (5)	0.591 (5)
(II), βXyl*p*	13.9 (10)	6(5)	0.551 (11)	0.131 (10)	0.535 (11)
(III), βGal*p*	4.84 (19)	28.0 (3)	0.595 (2)	0.049 (2)	0.593 (2)
(III), βGlc*p*	11.9 (2)	341.3 (13)	0.558 (2)	0.116 (2)	0.546 (2)
(IX), βXyl*p*	8.17	36.4	0.5795	0.0824	0.5737
(*X*), βGal*p*	5.89	346.7	0.5824	0.0597	0.5793
(XI), βGlc*p*	6.91	37.9	0.5972	0.0718	0.5928

† No s.u. values were provided in the original reports for (III), (IX), (X) and (XI).

Table 4
Comparison of φ' and ψ' glycosidic torsion angles in several β-(1→4)-linked disaccharides.

See *Comment* for literature references to individual disaccharide X-ray reports.

Compound	C2′—C1′—O1′—C4, φ' (°)	C1′—O1′—C4—C3, ψ' (°)
βGal(1→4)βXylOCH$_3$, (II)	156.4 (5)	94.0 (11)
βGal(1→4)βGlcOCH$_3$, (III)	153.8 (2)	78.4 (2)
βGal(1→4)αGlcOCH$_3$, (IV)	148.1 (1)	93.5 (1)
β-L-Gal(1→4)βGlcOCH$_3$, (V)	−146.19 (12)	111.14 (13)
βGal(1→4)αManOCH$_3$, (VI)	173.1 (2)	115.2 (2)
βGal(1→4)βAllOCH$_3$, (VII)	144.74 (10)	77.55 (13)
βGlc(1→4)βGlcOCH$_3$, (VIII)†	152.0	80.3

† No s.u. values were given in the original report.

cement parameters of adjacent atoms restrained to have similar U^{ij} values in the two disorder components.

H atoms were initially located from a difference Fourier map and subsequently included as riding atoms in geometrically idealized positions, with C—H = 0.98 (methyl), 0.99 (methylene) or 1.00 Å (methine) and O—H = 0.84 Å. For all H atoms, U_{iso}(H) = kU_{eq}(parent), where k = 1.5 for methyl groups and 1.2 for all other H atoms. Hydroxy H atoms were permitted to rotate but not tilt.

The assignment of the absolute configuration was based on the known configuration of the disaccharide from the synthesis. Refinement of the Flack x parameter [x = 0.6 (9); Flack, 1983] and Bayesian analysis of Bijvoet pairs of reflections [y = 0.4 (4); Hooft *et al.*, 2008] did not yield a conclusive analysis of the correct absolute configuration.

Data collection: *APEX2* (Bruker, 2008); cell refinement: *SAINT* (Bruker, 2008); data reduction: *SAINT*; program(s) used to solve structure: *SHELXS97* (Sheldrick, 2008); program(s) used to refine structure: *SHELXL97* (Sheldrick, 2008); molecular graphics: *XP* (Sheldrick, 2008), *POV-RAY* (Cason, 2003) and *DIAMOND* (Brandenburg, 2009); software used to prepare material for publication: *XCIF* (Sheldrick, 2008) and *publCIF* (Westrip, 2010).

Samples for synchrotron crystallographic analysis were submitted through the SCrALS (Service Crystallography at Advanced Light Source) program. Crystallographic data were collected at Beamline 11.3.1 at the Advanced Light Source (ALS), Lawrence Berkeley National Laboratory. The ALS is supported by the US Department of Energy, Office of Energy Sciences, under contract No. DE-AC02-05CH11231.

Supplementary data for this paper are available from the IUCr electronic archives (Reference: TP3005). Services for accessing these data are described at the back of the journal.

References

Boeyens, J. C. A. (1978). *J. Cryst. Mol. Struct.* **8**, 317–320.
Brandenburg, K. (2009). *DIAMOND*. Version 3.2e. Crystal Impact GbR, Bonn, Germany.
Bruker (2008). *APEX2* (Version 2010-7) and *SAINT* (Version 7.66A). Bruker AXS Inc., Madison, Wisconsin, USA.
Cason, C. J. (2003). *POV-RAY*. Version 3.6.2. Persistence of Vision Raytracer Pty. Ltd, Victoria, Australia.
Cremer, D. & Pople, J. A. (1975). *J. Am. Chem. Soc.* **97**, 1354–1358.
Flack, H. D. (1983). *Acta Cryst.* A**39**, 876–881.
Gruzman, A., Shamni, O., Yakir, M. B., Sandovski, D., Elgart, A., Alpert, E., Cohen, G., Hoffman, A., Katzhendler, Y., Cerasi, E. & Sasson, S. (2008). *J. Med. Chem.* **51**, 8096–8108.
Ham, J. T. & Williams, D. G. (1970). *Acta Cryst.* B**26**, 1373–1383.
Hooft, R. W. W., Straver, L. H. & Spek, A. L. (2008). *J. Appl. Cryst.* **41**, 96–103.
Hu, X., Pan, Q., Noll, B. C., Oliver, A. G. & Serianni, A. S. (2010). *Acta Cryst.* C**66**, o67–o70.
Jeffrey, G. A. & Takagi, S. (1977). *Acta Cryst.* B**33**, 738–742.
Nadanaka, S. & Kitagawa, H. (2008). *J. Biochem.* **144**, 7–14.

Ning, J., Zhang, W., Yi, Y., Yang, G., Wu, Z., Yi, J. & Kong, F. (2003). *Bioorg. Med. Chem.* **11**, 2193–2203.
Pan, Q., Noll, B. C. & Serianni, A. S. (2005). *Acta Cryst.* C**61**, o674–o677.
Pan, Q., Noll, B. C. & Serianni, A. S. (2006). *Acta Cryst.* C**62**, o82–o85.
Podlasek, C. A., Wu, J., Stripe, W. A., Bondo, P. B. & Serianni, A. S. (1995). *J. Am. Chem. Soc.* **117**, 8635–8644.
Schmidt, R. R. & Michel, J. (1985). *J. Carbohydr. Chem.* **4**, 141–169.
Sheldrick, G. M. (2008). *Acta Cryst.* A**64**, 112–122.
Spek, A. L. (2009). *Acta Cryst.* D**65**, 148–155.
Stenutz, R., Shang, M. & Serianni, A. S. (1999). *Acta Cryst.* C**55**, 1719–1721.
Takagi, S. & Jeffrey, G. A. (1977). *Acta Cryst.* B**33**, 3033–3040.
Takagi, S. & Jeffrey, G. A. (1979). *Acta Cryst.* B**35**, 902–906.
Taylor, M. E. & Drickamer, K. (2003). *Introduction to Glycobiology*, p. 34. Oxford University Press.
Tropper, F. D., Andersson, F. O., Grant-Maitre, C. & Roy, R. (1992). *Carbohydr. Res.* **229**, 149–154.
Voet, J. G. & Voet, D. (2011). *Biochemistry*, p. 380. New York: John Wiley & Sons Inc.
Westrip, S. P. (2010). *J. Appl. Cryst.* **43**, 920–925.
Wu, J. & Serianni, A. S. (1991). *Carbohydr. Res.* **210**, 51–70.
Zhang, W., Oliver, A. G. & Serianni, A. S. (2010). *Acta Cryst.* C**66**, o484–o487.